Research Article

Electropolishing of Additively Manufactured Ti-6Al-4V Surfaces in Nontoxic Electrolyte Solution

G. M. Tsoeunyane [1,2] **N. Mathe,**[1,2] **L. Tshabalala,**[2] **and M. E. Makhatha** [1]

[1]*Faculty of Engineering and Built Environment, Department of Metallurgy, University of Johannesburg, Johannesburg, South Africa*
[2]*National Laser Centre, CSIR, Pretoria, South Africa*

Correspondence should be addressed to G. M. Tsoeunyane; m.tsoeunyane.mg@gmail.com and M. E. Makhatha; emakhatha@uj.ac.za

The reduction of surface roughness on additively manufactured components has become a critical factor in engineering applications. This paper reports the electropolishing of additively manufactured Ti-6Al-4V by powder bed selective laser melting (SLM) using a nontoxic electrolyte solution. The results have shown that the salt-based electrolyte can be used to electropolish titanium alloys. The surface waviness of the as-built Ti-6Al-4V alloy was reduced by five times the average roughness of the as-built specimen. The minimum surface roughness obtained was $9.52\,\mu$m. The specimens were characterized by scanning electron microscope, Gwyddion software, and electrochemical impedance spectroscopy (EIS) to evaluate the surface morphology, surface profile, and charge transfer resistance. The X-ray photon spectroscopy (XPS) and X-ray diffraction (XRD) spectroscopy were used to characterize the surface chemistry of the specimen. The XPS and XRD showed TiO_2 as the significant component on the surface of Ti-6Al-4V, and the atomic percentage on the surface increased after electropolishing. In addition, the EIS data indicated the high charge transfer resistance of the electropolished specimen, which shows the growth formation of the oxide layer.

1. Introduction

Additive manufacturing (AM) has been recognized as a game-changer in the manufacturing sector [1, 2]. Despite AM capabilities and advantages over traditional manufacturing techniques, surface roughness is an unresolved challenge [3] that limits the broad adoption of additive manufacturing (AM) techniques/processes [4, 5]. According to Gisario et al., surface roughness results from the geometric error discrepancy of the intended final product and unmelted powders [6].

Mechanical, chemical polishing, electropolishing with mixture of mineral acids, and laser surface treatment techniques have been reported as posttreatment processes for laser-built components to reduce the surface roughness of the resulting parts. The postprocessing techniques include short peening [7], low plasticity burnishing [8], laser shock processing [9], surface laser remelting [10], and deep cryogenic treatment [11]. All these techniques are complex and require computer-aided designs. Chemical polishing is one of the alternative processes to post-treat additively manufactured parts. The process works well with complex design shapes [12]. However, the metal removal or dissolution on the surface is not uniform as reported by Balyakin et al. [13].

The alternative to getting uniform surface of additively manufactured parts is by electropolishing [14]. Electropolishing (EP) is a chemical removal of the metal depending on the local charge density, binding energy, and mass transfer on the polished surface of the metal [15]. The electropolishing principle was first discovered by Faraday in the 19th century. This is a nonconduct and destructive process [16]. Zhang et al. [17] attempted to electropolish as-built Ti-6Al-4V parts with an electrolyte containing chloride concentration at room and a current density of $0.5\ \text{Acm}^{-2}$. The surface roughness of the workpiece was decreased to

75% and a weight loss rate of 4.9% at the chloride concentration of $0.4\,molL^{-1}$. The results further indicated that the formation of stable TiO_2 on the surface improved the corrosion resistance significantly. The magnesium chloride was used as the source for chloride ions. According to Zhang et al., the workpiece's resultant surface roughness and gloss finish were unsatisfactory.

The conditions and mechanisms for electropolishing had previously been published. Wei Han et al. [16] summarised the fundamental aspects and recent developments in electropolishing. The factors included electropolishing temperature, electrolyte composition, current-voltage effect, rotation speed, and time. Electropolishing occurs by two effective mechanisms, which are anodic levelling (macro-smoothing) and anodic brightening (microsmoothing) [15] as opposed to etching of the surface. Anodic levelling happens because of different local charge distributions where the peaks on the surface preferentially dissolve while microsmoothing occurs because of the suppressed surface defects and crystallographic orientation in the dissolution process.

The electropolishing of as-built parts by laser with mixed metal salts (MMSs) in an organic electrolyte has not been extensively studied to the author's best knowledge. Therefore, the current study reports an attempt to electropolish as-built additively manufactured Ti-6Al-4V parts by MMS organic electrolyte. We present the electropolishing media that does not involve a mixture of mineral acids but rather a mixture of salts and organic solvents. The electropolishing media is designed to have high viscosity, ensuring near-uniform heat distribution within the electropolishing cell. Moreover, the viscous fluid will ensure the blockage of valleys on the surface of the alloy and allow the current concentration on the peaks, which will assist dissolution.

2. Experimental

2.1. Surface Preparation of Ti-6Al-4V.
The 10 cm as-built Ti-6Al-4V SLM cylindrical rods of 1.0 cm diameter were obtained from CSIR, South Africa. The specimens were cut into 2.0 cm length from the rod for mechanical polishing and electropolishing tests. The specimens' surfaces were mechanically grounded with 200, 400, 800, and 1000 grit SiC paper sequentially and then washed with distilled water and degreased with acetone. The grinding of the surface was to remove any oxides that might have formed during processing. For electropolishing, as-built samples were used. The samples were washed with distilled water and used without any processing.

2.2. Mixed Metal Salt-Based Electropolishing Media for Ti-6Al-4V SLM Built Alloy.
Electropolishing was carried out on the as-built Ti-6Al-4V specimen with a direct current (DC) supply in a two-electrode system with applied current of $0.2\,Acm^{-2}$. The cell housing was a 300 ml Pyrex beaker with two electrodes, an electrolyte solution, and a 250 mm long stainless-steel Teflon-coated rod with an electrode holder at the end. The electrode holder is sealed to allow only the exposed surface to be in contact with the solution. As-built titanium specimen and pure copper plate were used as anode and cathode, respectively. The copper plates were cut into 100 mm × 40 mm × 20 mm. Pure copper was chosen to be the cathode electrode because it provides a nucleation site for dissolved hydrogen gas (H2), thereby speeding up the removal of the gas from the system, increasing the quality of the surface finish. A 5 mm average working distance was kept between the electrodes in the cell. TOPWARD dual-tracking DC power supply 6303 A was used to supply direct current to the system. A hotplate/stirrer was used to rotate the stirrer bar and maintain temperature.

The temperature of the electropolishing electrolyte was kept at $30.0 \pm 2°C$ while stirring with a magnetic stirrer. The stirring rate was maintained at 400 rpm. The main parameters for electropolishing are shown in Table 1. Only the electrolyte composition was varied while current, temperature, and electropolishing time were kept constant. Before electropolishing, a three-electrode system consisting of a saturated calomel electrode (SCE), as-built Ti-6Al-4V, and graphite were used as a reference, working, and counter electrode to establish the corrosion potential (Ecorr) of Ti-6Al-4V by linear polarization (LPR). The Ecorr value was then used to estimate the current that must be supplied to the working electrode in the electropolishing cell to ensure the dissolution. The system was polarized with $10\,mVs^{-1}$ in the potential range of −10 V to 10 V. The LPR was performed on Bio-Logic SP-150 potentiostat. Instead of recording the classical potential current density during electropolishing, a $0.2\,Acm^{-2}$ of current density was imposed for different periods.

2.3. Surface Morphology and Elemental Characterization.
The morphology of the titanium specimens was observed using a scanning electron microscope (SEM) (Vega, Tescan) equipped with Oxford energy dispersive X-ray (EDX) analysis. A Gwyddion 2.9.32 software was coupled with SEM images and used to characterize the waviness and roughness of the surface on titanium specimens. The 18-pixel average coverage was selected from the software in a straight line, and the average of three values was reported as the final value The roughness parameters such as average roughness (Ra), the average maximum height of the profile (Rz), root mean square roughness (Rq), mean spacing of profile irregularities (Sm), average wavelength of the profile (λa), and average waviness (Wa) were obtained. The original 3D surface plots of the specimens were then reconstructed. In addition, the chemical composition layer was analysed using X-ray photon spectroscopy (XPS). The XPS was used to observe if the oxide layers on the surface of Ti-6Al-4V change with electropolishing and identify major peaks on the surface. The X-ray diffraction (XRD) spectrometer Rigaku Ultima IV with the scan speed of 1.0 deg/min and voltage of 40 kV was further used to characterize the surface of electropolished specimen.

2.4. Electrochemical Impedance Spectroscopy (EIS).
The EIS measurements of each specimen were carried out using a Bio-Logic SP-150 potentiostat. A three-electrode system was

TABLE 1: Electropolishing parameters.

Parameters	Electrolyte 1	Electrolyte 2	Electrolyte 3
Triethanolamine	180 ml	180 ml	180 ml
Perchloric acid	10 ml	—	—
Sodium flouride (NaF)	1.17%	1.17%	2%
Ammonium flouride (NH4F)	5%	10%	10%
Oxalic acid	16%	16%	16%
Ethanol	15 ml	15 ml	15 ml
Current density	$0.2\,Acm^{-2}$	$0.2\,Acm^{-2}$	$0.2\,Acm^{-2}$
Time	30 min	30	30
Temperature	$30.0 \pm 2°C$	$30.0 \pm 2°C$	$30.0 \pm 2°C$

used where titanium specimen, saturated calomel electrode (SCE), and graphite rod were used as working, reference, and counter electrodes, respectively, in $0.5MH2SO4$ at $30.0 \pm 2°C$. Before EIS measurements, the Ti-6Al-4V specimens were let to corrode freely to attain a stable open circuit potential (OCP). The electrode open circuit potential vs. SCE was stable after 30 minutes. Electrochemical impedance spectroscopy (EIS) was conducted to characterize the nature of the oxide layers formed on the titanium specimen after electropolishing. The experiment was run in the frequency range of 20 KHz to 0.1 Hz with the sinus amplitude potential of 10.0 mV. The potential range of 0 to 10 V was used because of the nonconductive layer of oxide that formed on titanium. The Nyquist diagram was obtained using the Z-fit EC-lab software. The EIS parameters were then determined, and an electrical equivalent circuit (ECC) model was proposed.

3. Results and Discussion

3.1. Linear Polarization (LPR) and Open Circuit Potential (OCP) of Ti-6Al-4V. The polarization of Ti-6Al-4V was carried out to obtain the corrosion potential or potential at which the specimen would dissolve during electropolishing. The experiment was carried out instead of classical current-potential curves used in electropolishing. Figures 1 and 2 show the OCP and LPR of the as-built Ti-6Al-4V in $0.5MH2SO4$. The OCP of as-built Ti-6Al-4V stabilizes at a higher positive potential. This is indicative of the high corrosion resistance of Ti-6Al-4V. At the beginning of LPR, a sharp increase in current density J was observed, followed by a slow increase with potential (V). An initial region with a sharp increase was in the negative region of current density vs. potential, signifying the electrolyte media's gas evolution. The anode started to dissolve at the slow increase in the J region. The LPR parameters Ecorr, Icorr, and Rp were 168.9 mV, 6.814 32 $\mu A/cm^2$, and 3828 Ohm·cm^2, respectively. The high positive corrosion potential of Ti-6Al-4V was because of the resistivity nature of titanium alloys to dissolution in aggressive media. Titanium alloys form a stable TiO_2 on their surface, which passivates the alloy, preventing dissolution. In this case, the oxides were formed during the manufacturing of the alloy. Characterizing the oxides on the as-built Ti-6Al-4V alloy proved challenging in this work because of the specimen's roughness caused by
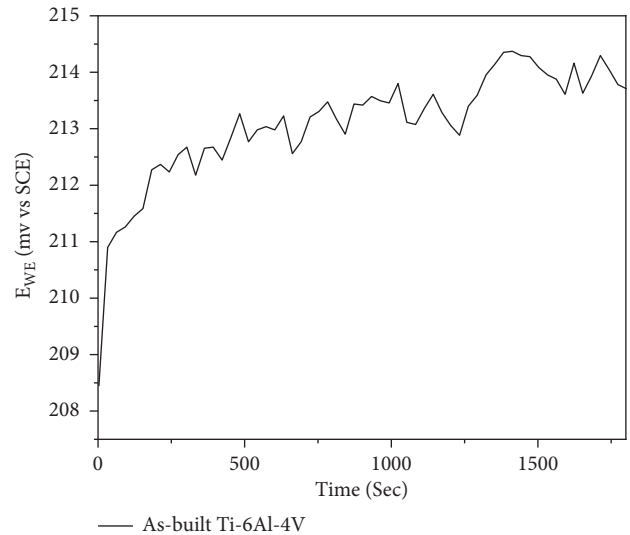

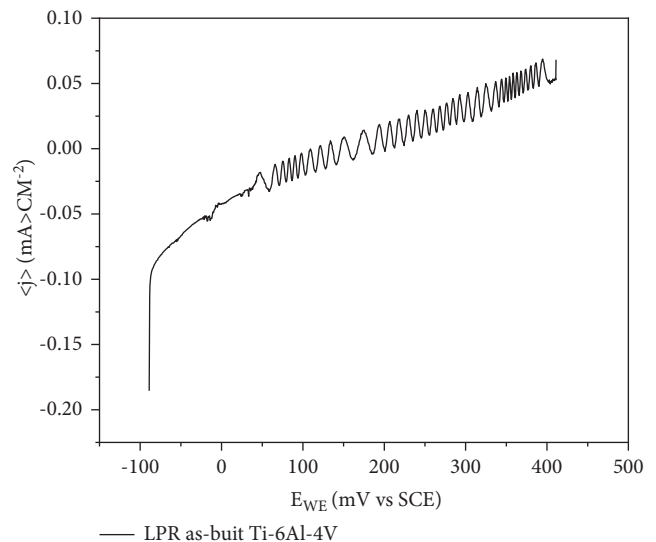FIGURE 1: Open circuit potential of as-built Ti-6Al-4V in $0.5MH2SO4$.

FIGURE 2: LPR of as-built Ti-6Al-4V in $0.5MH2SO4$.

unmelted powders that adhered to the surface. The SEM image of the as-built Ti-6Al-4V alloy is shown in Figure 3.

3.2. Effect of Electrolyte Composition. During electropolishing, the effect of electropolishing was investigated. Initially, an electrolyte with perchloric acid was used as the component of the solution (electrolyte-1). The results obtained were satisfactory, but the mass-loss rate was higher at 30 minutes with the applied current of 0.2 A/cm^2. Both time and current were kept constants for all different electropolishing media. The high mass-loss rate was attributed to the applied current and chemical process combination. The chemical process was due to the reaction of Ti with chloride (Cl-) and fluoride (F-) ions, as shown by equations (2) and (3). Equation (1) shows a simplified dissolution of titanium.
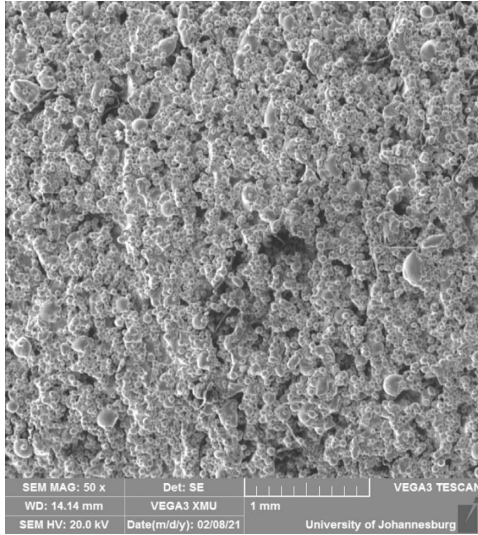
FIGURE 3: The SEM image showing the as-built Ti-6Al-4V with unmelted powders adhered to the surface.

The reactions towards Ti dissolution were additive in terms of mass loss. Four of each anionic species were reacting with respective titanium, increasing the rate of dissolution. The pit-like formation was observed on the specimen electropolished with the electrolyte 1 combination.

$$Ti \longrightarrow Ti^{4+} + 4e^-, \tag{1}$$

$$Ti^{4+} + 4Cl^- \longrightarrow TiCl_4, \tag{2}$$

$$Ti^{4+} + 4F^- \longrightarrow TiF_4. \tag{3}$$
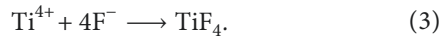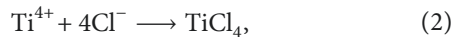
It is stated that the film TiCl4 can be problematic if not removed quickly because the film can passivate titanium there by resulting in an inhomogeneous polished surface [18]. Therefore, a strong stirring force is required in an electropolishing cell to remove the film. The 400 rpm stirring was employed, which we believe was able to remove the film.

3.3. Morphology of As-Built, Mechanically Polished, and Electropolished Ti-6Al-4V Specimen Surface.

Figure 4 displays the SEM images of the original surface profiles of as-built and mechanically polished Ti-6al-4V alloy. The titanium alloy surface is spontaneously covered with a natural oxide film in the air at room temperature. The film is only a few nanometres thick and transparent. Therefore, the natural oxide film formed on the grinded surface resulted in scratches, as shown in Figure 4(b). The average surface roughness of the ground specimen (Ra) was $9.12\,\mu m$, root mean square average (Rq) was $11.64\,\mu m$, and mean spacing of average irregularities (Sm) was $33.81\,\mu m$. The as-built specimen in Figure 4(a) has Ra, Rq, and Sm of $45.22\,\mu m$, $57.03\,\mu m$, and $53.84\,\mu m$, respectively. From the results, as expected, the roughness value of mechanically polished specimen is five times less than the one for as-built specimen.

The surface roughness of as-built specimen is the result of balling where the unmelted powders adhered to the built substrate. Mechanical polishing attains a smoother surface with low surface roughness but left the scratch marks on the surface. The balling phenomenon is shown in Figure 4(a). The surface topography has a major impact on the performance of parts in application. The actual 3D surface profiles of the two specimens were constructed. It is clear from Figure 4(c) that the as-built specimen has the sharp peaks across the whole surface compared with mechanically polished specimen in Figure 4(d). The removal of balling effect in Figure 4(a) resulted in a smooth 3D plot for mechanically polished specimen.

The electropolishing of as-built Ti-6Al-4V alloy was carried as a post-processing method towards the better surface finish profile. The importance of electropolishing against other postprocessing techniques is that complex designed shape parts can be polished easily as compared with other processes. In addition, the mass loss on the samples can be regulated despite the complexity of chemistry and electricity combination in the process. The electropolishing parameters are as shown in Table 1. The three different electrolyte media were used; the first polishing electrolyte contained a mineral acid perchloric acid. The comparison on the results was made.

All the electropolished surfaces from three different solutions showed an even surface on the SEM micrograph compared with a mechanically polished specimen. The phenomenon can be attributed to the uneven distribution of the current during electropolishing. Theoretically, the current distribution on the surface during electropolishing depends on the surface texture, composed of surface roughness (microroughness) and waviness (macroroughness).

The current initially concentrates on the high peaks protruding from the valley; therefore, the metal solution film is formed during electropolishing depending on the electrolyte, which acts as a capacitor. The high peaks start to dissolve when the current passes through the anode. The formed metal solution film limits or controls the amount of current passed to the metal surface, regulating the amount of alloy lost during the electropolishing process.

Titanium alloys are generally known to have high oxygen affinity, forming a stable oxide film rutile resistant to dissolution. In this work, during the electropolishing of Ti-6Al-4V alloy, there was uncontrolled oxide film growth despite using an electrolyte solution with less water content. Triethanolamine was used as a major solvent in the electrolyte formulation because of its low viscosity as compared with water or other low molecular weight alcohols which ensured the even distribution of heat within the solution during the process.

The average surface roughness after electropolishing of Ti-6Al-4V alloy in electrolytes 1, 2, and 3 was five times less than the average roughness of as-built specimen. The Ra in electropolished samples was 80% reduced from the as-built sample. The results show the success of the electropolishing process despite the imperfections of the surface obtained after electropolishing. In Figure 5(a) where electrolyte 1 was used, the signs of pitting of the surface is observed. The pitting was due to the strong action of chloride and flouride ions against the alloy, as shown by equations (2) and (3). In

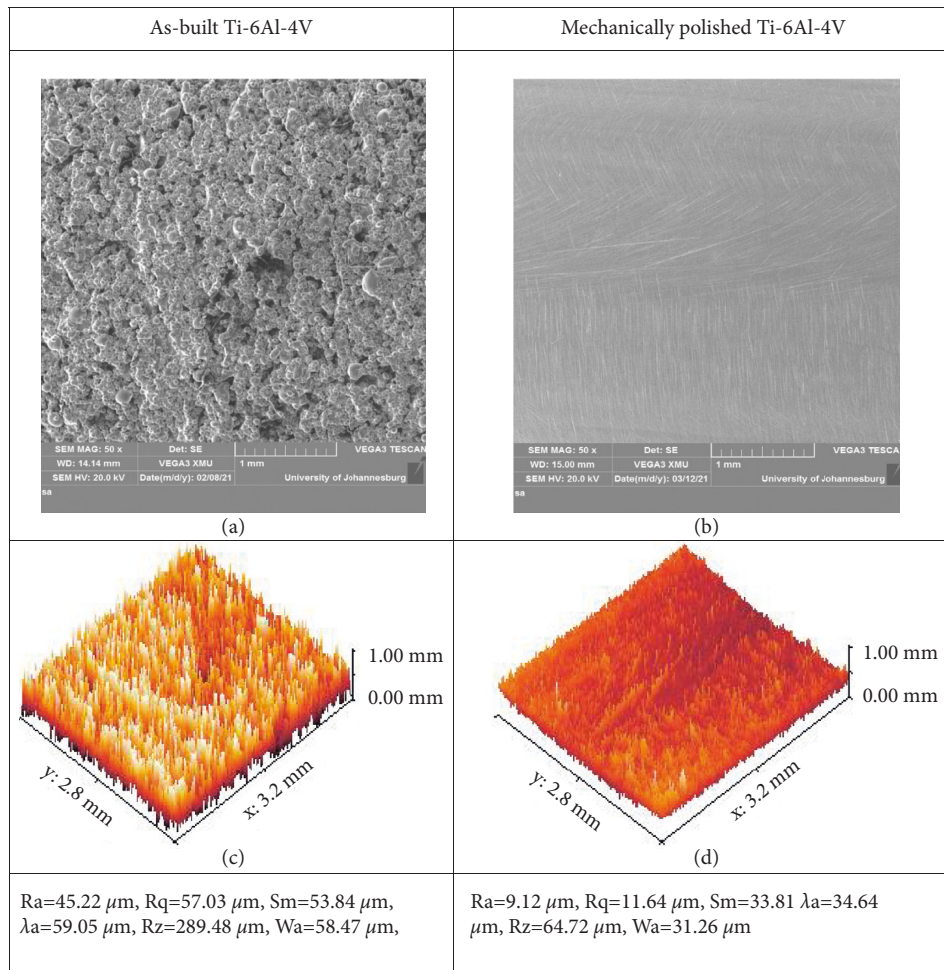| As-built Ti-6Al-4V	Mechanically polished Ti-6Al-4V
(a)	(b)
(c)	(d)
Ra=45.22 μm, Rq=57.03 μm, Sm=53.84 μm, λa=59.05 μm, Rz=289.48 μm, Wa=58.47 μm,	Ra=9.12 μm, Rq=11.64 μm, Sm=33.81 λa=34.64 μm, Rz=64.72 μm, Wa=31.26 μm

FIGURE 4: The SEM micrographs of (a) as-built and (b) mechanically polished and original surface profile of (c) as-built and (d) mechanically polished Ti-6Al-4V SLM built specimens.

the electrolytes where perchloric acid was absent, there were no pits observed. However, the surface average surface roughness (Figure 5) was comparable in all specimens electropolished by electrolyte 1, 2, and 3, respectively. It should be noted that the current density of 0.2 Acm^{-2} was used in all experiments with the exposure time of 30 minutes as opposed to traditional varying of applied current or voltage to the anode. During postprocessing techniques, considerable amount of mass of the specimen is lost to attain desired surface finish profile and shape. In this work, the maximum amount of mass lost during process was less than 1%.

Despite the considerable success of the process in surface roughness reduction of the specimen, the bright, smooth, and flat surface without scratches were not obtained. The pits were avoided in electrolyte 2 and 3, respectively (shown in Figure 6) where the mineral acid was not incorporated. The stair-stepping and balling on the samples were levelled but the samples did not show bright surfaces after electropolishing. The electropolishing process enables the removal of material from the anode and simultaneously allows the formation of oxide layers to avoid etching of the metal. The formed oxide layer on Ti-6Al-4V alloy is significantly stable

and resistant to dissolution. In addition, the oxide layer is nonconductive and disrupts the direct current (DC) on the anode, therefore, resulting in uneven surface formation on the Ti-6Al-4V alloy during electropolishing. As the result, in this work, the uneven surface with pit formation (Figure 6(a)) and waviness on the electropolished surface is observed despite improved average surface roughness.

The surface texture of the specimen was analysed and quantified using SEM image coupled with Gwyddion software. Figures 6(d), 6(e), and 6(f) show the 3D plot surface specimen electropolished with electrolyte 1, 2, and 3. It can be observed that the 3D plot surfaces of all specimens are comparable; this implies that the method of material removal from the Ti-6Al-4V SLM built specimen was the same throughout. The surface texture parameters are listed in Figure 6. The electropolished surfaces showed a low average roughness value because the microvalleys and scratches were removed despite indicating an uneven surface compared with mechanically polished.

3.4. Chemical Composition of the Surface Layer of As-Built, Mechanically Polished, and Electropolished Ti-6Al-4V Specimen. The XPS survey spectrum of the surface layer of the
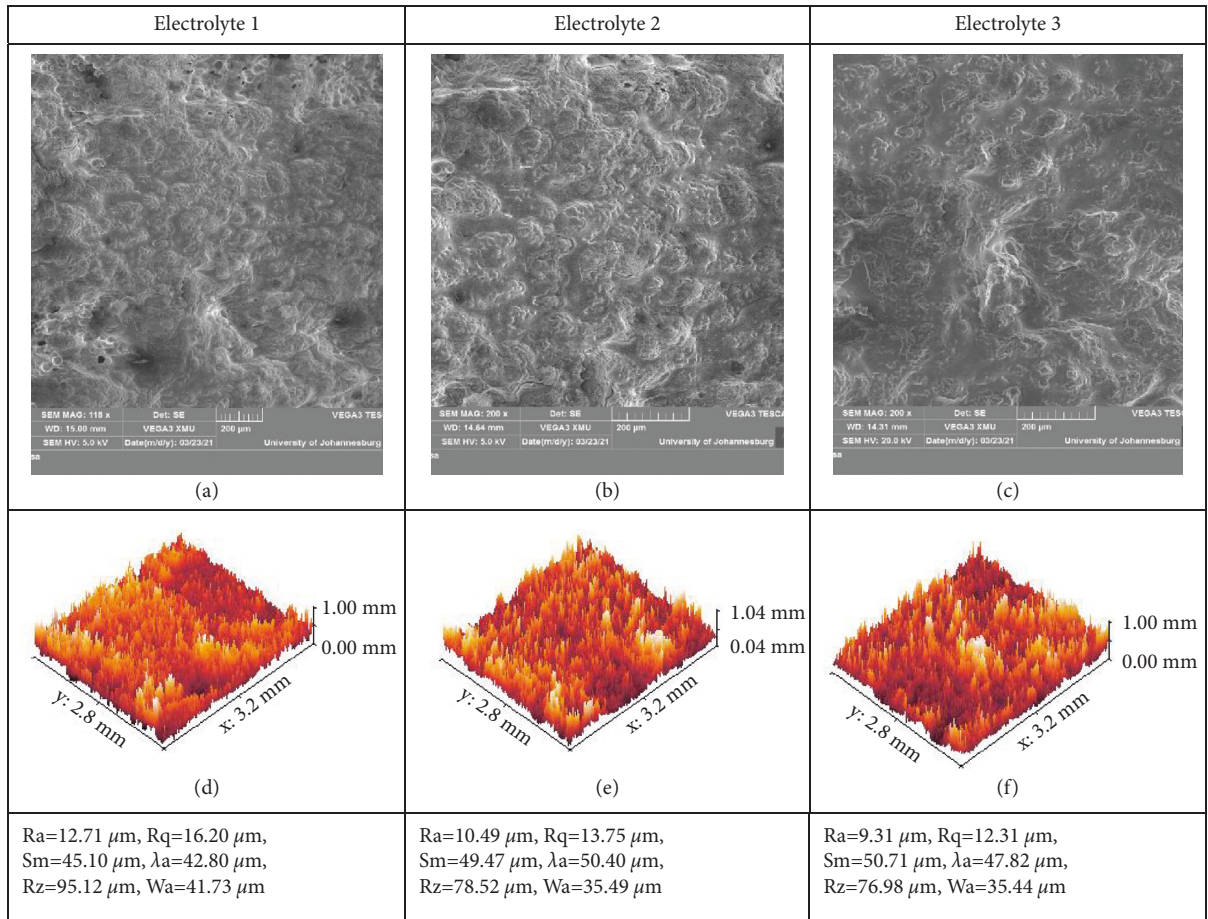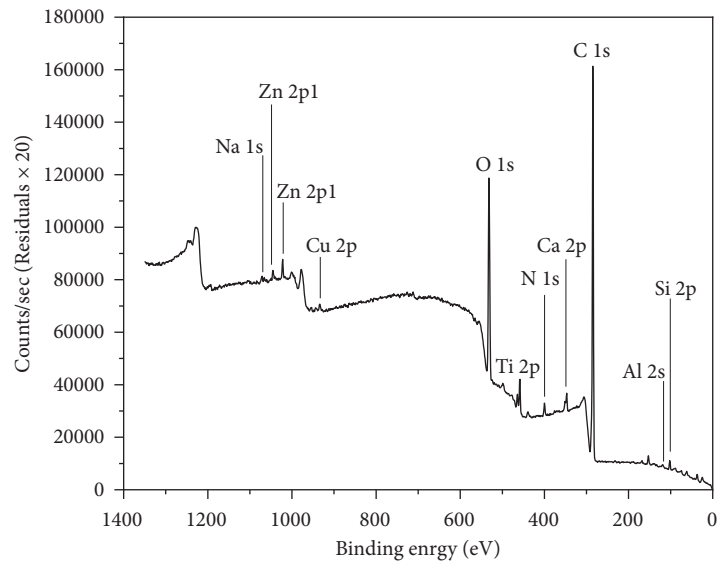
Electrolyte 1	Electrolyte 2	Electrolyte 3
(a)	(b)	(c)
(d)	(e)	(f)
Ra=12.71 μm, Rq=16.20 μm, Sm=45.10 μm, λa=42.80 μm, Rz=95.12 μm, Wa=41.73 μm	Ra=10.49 μm, Rq=13.75 μm, Sm=49.47 μm, λa=50.40 μm, Rz=78.52 μm, Wa=35.49 μm	Ra=9.31 μm, Rq=12.31 μm, Sm=50.71 μm, λa=47.82 μm, Rz=76.98 μm, Wa=35.44 μm

FIGURE 5: The SEM images electropolished Ti-6Al-4V specimen in (a) Electrolyte 1, (b) Electrolyte 2, (c) Electrolyte 3 and original 3D surface profile of specimen (d), (e), and (f) in Electrolyte 1, 2 and 3, respectively The SEM images electropolished Ti-6Al-4V specimen in (a) Electrolyte 1, (b) Electrolyte 2, (c) Electrolyte 3 and original 3D surface profile of specimen (d), (e), and (f) in Electrolyte 1, 2 and 3, respectively.

as-built, mechanically polished, and electropolished specimens (electrolyte 3) is presented in Figure 5. It is observed that the oxide film mainly contained O, C, Ca, Na, N, Zn, Cu, Al, Si, and Ti. Ti and O are the dominant elements of titanium oxide. This is observed in all the three specimens. C and N originated from the air or electrolyte. The other elements might have originated from the X-ray within the sample despite the possibility being rare [19]. Al in Ti-6Al-4V occurs as Al_2O_3 which is only 6%; V is even lower; therefore, it becomes difficult to detect the binding energy on the XPS spectra. Therefore, the focus of the 2p spectrum was mainly of Ti in this study.

The high-resolution XPS spectrum of the Ti 2p region is shown in Figure 7. The Ti 2p photoemission signal splits into two peaks in Figure 7(a) as-built, Figure 7(b) as mechanically polished, and Figure 7(c) as electropolished, respectively. At the energy of 458.3 eV, the first one is attributed to Ti 2p3/2 (IV), and the second one, at the energy of 465 eV, is attributed to Ti 2p1/2 (IV) of the as-built specimen. The photoemission signal splits of mechanically polished were observed at 458.6 eV attributed to Ti 2p3/2 (IV) and 466 eV attributed to Ti 2p1/2 (IV), while signals for electropolished were observed at 485.3 eV attributed to Ti 2p3/2 eV (IV) and 468 eV attributed to Ti 2p1/2 (IV). The presence of Ti (IV) suggests that TiO_2 was the constituent of the oxide film [17]. Table 2 shows

the peak analysis counts of atomic percentages from the high-resolution XPS spectrum. It can be observed that the atomic % of the identified titanium oxide increased in the electropolished specimen compared with the mechanically and as-built specimens. The increase in the oxide layer signifies the growth of the oxide layer during electropolishing, which is essential for the corrosion resistivity of titanium alloy. Table 3 shows the literature values for the Ti 2p3/2 spectrum, which are comparable to the experimental data shown in Table 2. The oxide layer on the surface was determined to be rutile as shown in the XRD spectrum (Figure 8).

3.5. Electrochemical Analysis of Mechanically Polished and Electropolished Ti Alloys.

It is well known that Ti alloys are highly resistant to corrosive media due to the oxide layer. On the other hand, the electropolishing process is expected to alleviate the corrosion protection of species. During electropolishing, it is theorized that the removal of materials from the surface and the formation of protective oxide layers should be uniform to avoid pitting that could occur on the surface and keeping the parts shape close to original [20]. Since the oxide layers formed on the Ti-6Al-4V alloy are not conductive, this will ensure the protection of the alloy

(a)
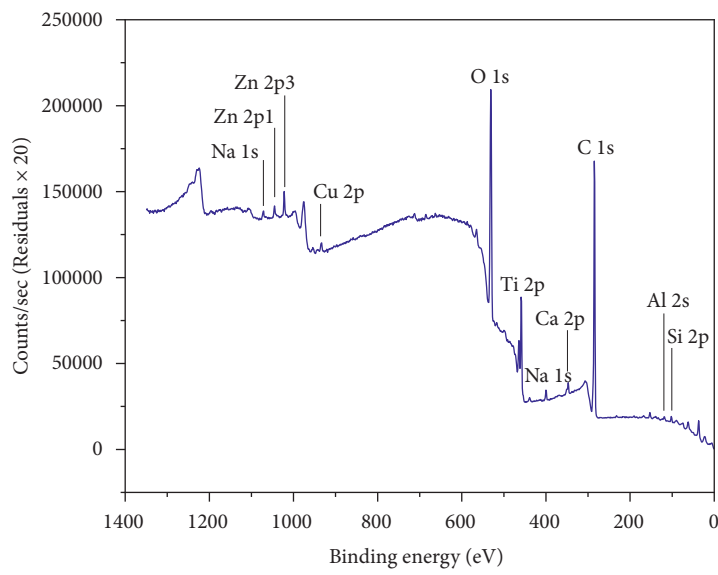
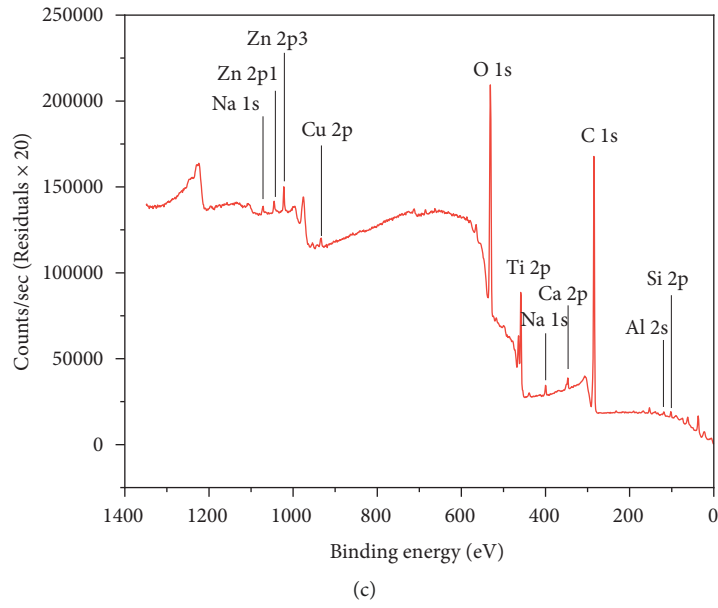
(b)

FIGURE 6: Continued.

(c)

FIGURE 6: The SEM images electropolished Ti-6Al-4V specimen in (a) electrolyte 1, (b) electrolyte 2, and (c) electrolyte 3 and original 3D surface profile of specimen in (d) electrolyte 1, (e) electrolyte 2, and (f) electrolyte 3.
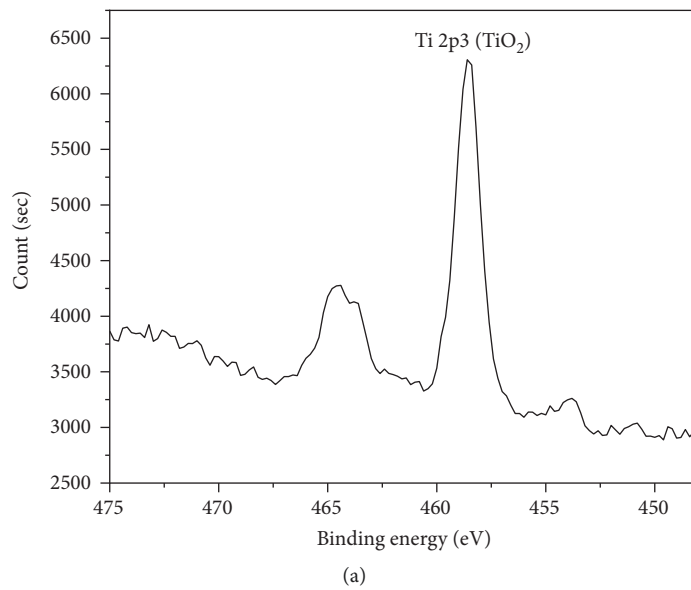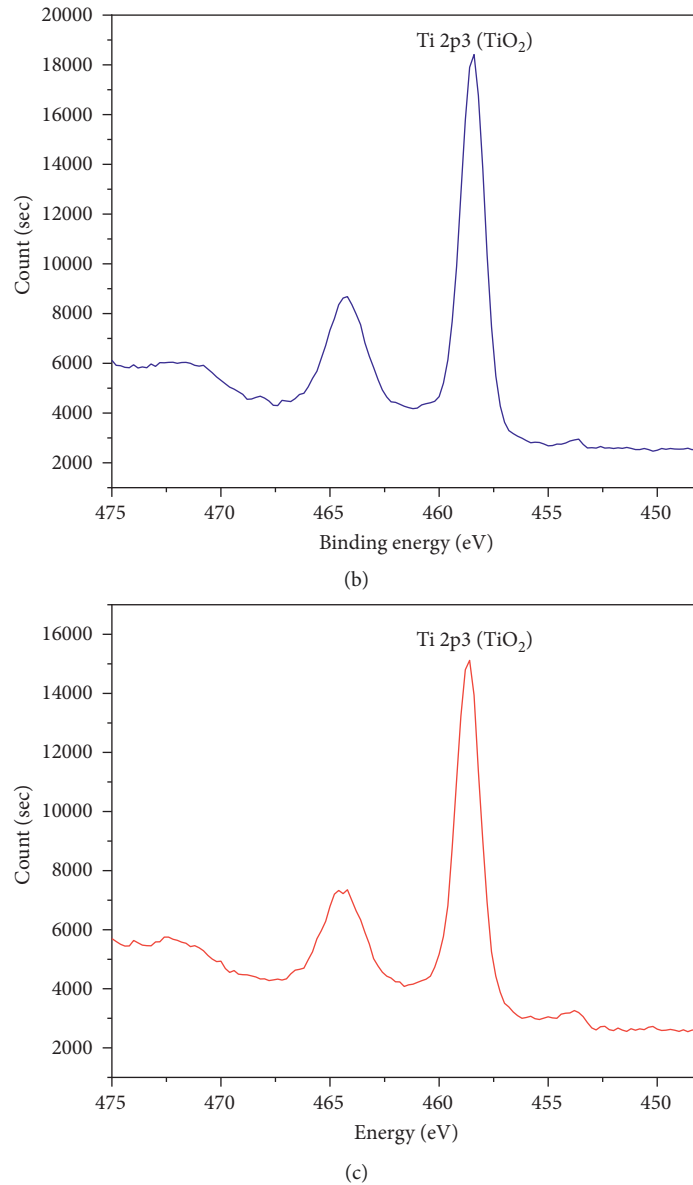

(a)

FIGURE 7: Continued.

(b)

(c)

FIGURE 7: High-resolution XPS spectrum showing Ti 2p3/2 of (a) as-built, (b) mechanically polished (MP-1), and (c) electropolished (ER-7) Ti-6Al-4V SLM built specimens.

TABLE 2: Ti 2p peak band energy and full-width-at-height-maximum (FWHM) of (a) as-built, (b) mechanically polished, and (c) electropolished (electrolyte 3) Ti-6Al-4V SLM built specimens.

Sample ID	Compound	Ti 2p3/2 (eV)	Atomic %	FWHM (eV)
As-built	Ti (IV) oxide	458.3	1.5	1.3
Mechanically polished	Ti (IV) oxide	458.6	1.7	1.3
Electropolished	Ti (IV) oxide	485.3	6.4	1.3

TABLE 3: Literature values for band energy of Ti 2p3/2 spectra.

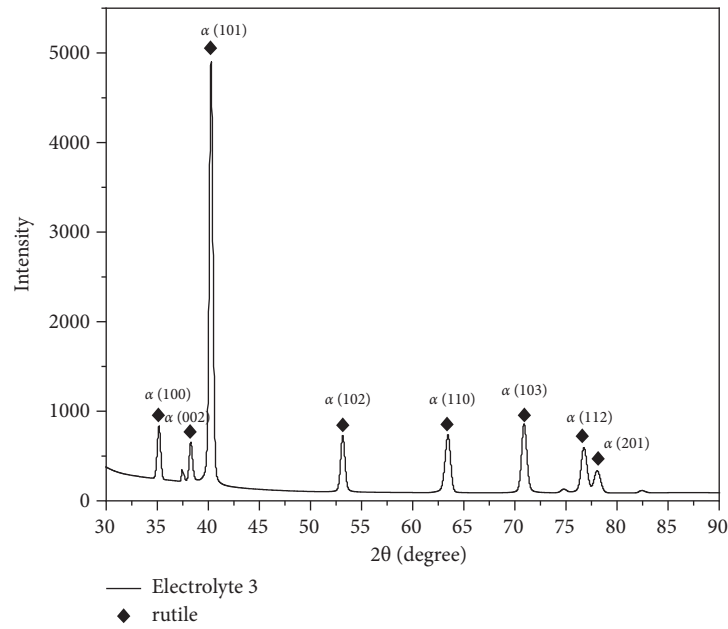| Compound	Ti 2p3/2 (eV)	FWHM Ti 2p3/2 (eV)
Ti (0) (a)	453.7	0.7
Ti (IV) oxide (rutile)	458.5	1.0
Ti (IV) oxide (anatase)	458.6	1.0

FIGURE 8: The XRD spectrum of SLM built Ti-6Al-4V specimen electropolished with electrolyte 3.
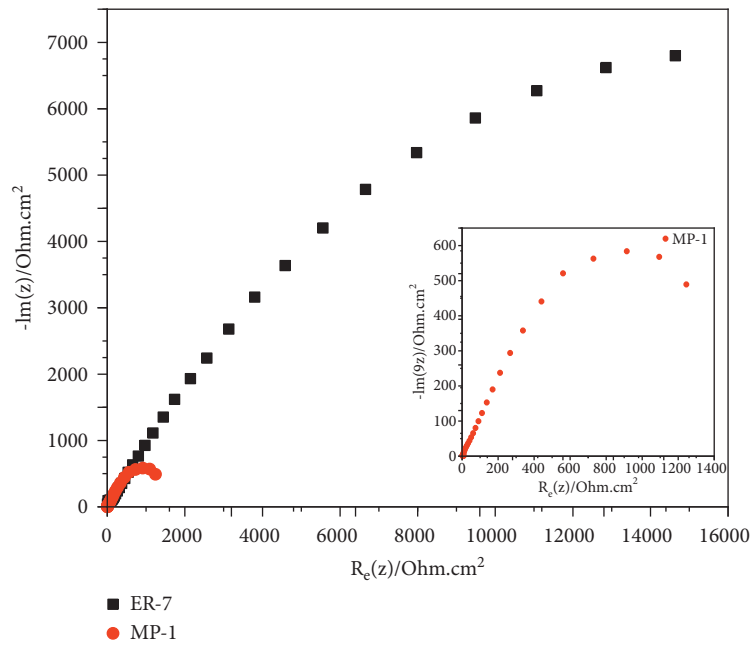

FIGURE 9: The EIS spectrum of mechanically polished and electropolished SLM manufactured Ti-6Al-4V alloy in 0.5MH2SO4 at 30.0°C.
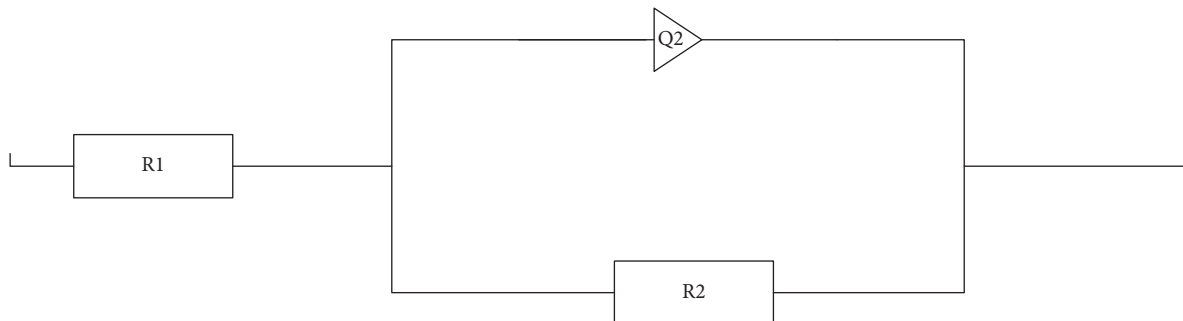

FIGURE 10: The electrical equivalent circuit model of Ti-6Al-4V in 0.5MH2SO4 at 30.0°C.

TABLE 4: The EIS parameters of mechanically polished and electropolished Ti-6Al-4V SLM built specimens.

Sample	R1/ Ohm	R2/ Ohm	Q2/ F.s$^{(a-1)}$	a_2
Mechanically polished	1.19	1352	1.18e-3	0.581
Electropolished (electrolyte 3)	1.19	18644	3.11e-5	0.491

against harsh environments. For electrochemical test in this work, sulphuric acid (H_2SO_4) was chosen to provide harsh environment to Ti-6Al-4V SLM built specimens.

The electrochemical impedance spectroscopy of mechanically polished and electropolished Ti-6Al-4V immersed in $0.5MH_2SO_4$ is shown in Figure 9 in the form of a Nyquist plot. The equivalent electric circuit (EEC) model is proposed to fit the measured impedance data in Figure 10. The chi-square value was used to evaluate the fitting confidence. Generally, the lower the chi-square value is, the more precise the proposed model is. The value was in the order of 10−2, and the corresponding electrical parameters constant phase element (CPE) and resistance (R) were obtained from EIS data as shown in Table 4 where R1 is solution resistance, R2 is charge transfer resistance, and Q2 and a_2 are parameters associated with constant phase element and.

Figure 9 shows the Nyquist plot of Ti-6Al-4V alloy in 0.5 M sulphuric acid; the plot of both curves does not show capacitative behaviour since the value of parameter a_2 is not close to unity from the modelling of the circuit [21]. This implies that the oxide layer formed on the alloy surface is not conductive, therefore, protecting the alloy from corroding. The electropolished specimen showed a high charge resistance of 18644 ohms, while the mechanically polished specimen had a relatively lower charge resistance of 1352 ohms. The high charge transfer resistance implies a more stable and thick oxide on the alloy surface, inhibiting the dissolution. Therefore, in this study, electropolishing does enable the growth of the oxide layer and inhibits the specimen from corroding. During electropolishing, the electrolyte is constantly stirred. The stirring of the electrolyte enables oxygen concentration increases in the solution which reacts with titanium ions on the surface of the alloy thereby for the oxide layer.

4. Conclusions

(i) The proposed electrolyte polishing media effectively reduces the surface roughness of as-built Ti-6Al-4V.

(ii) The minimum values of Ra = 9.31 μm, Rq = 12.31 μm, Sm = 50.71 μm, λa = 47.82 μm, Rz = 76.98 μm, and Wa = 35.44 μm were obtained after electropolishing in electrolyte 3.

(iii) The XPS data revealed the formation of TiO_2 on the surface after electropolishing. The difference with mechanically polished specimen is the high atomic percentage present in the electropolished specimen.

(iv) The EIS data showed increased charge transfer resistance, showing that the oxide layer increased in thickness.

(v) The XRD data also showed the presence of oxide layer, rutile on the surface, and α phase. The β phase was not present on the diffractogram.

Conflicts of Interest

The authors declare that there are no conflicts of interest in this work.

References

[1] S. O. Onuh and Y. Y. Yusuf, "Rapid prototyping technology: applications and benefits for rapid product development," *Journal of Intelligent Manufacturing*, vol. 10, no. 3/4, pp. 301–311, 1999.

[2] L. Kumar, V. Kumar, and A. Haleem, "Rapid prototyping technology for new product development," *Int. J. Innov. Sci. Eng. Technol*, vol. 3, no. 1, pp. 287–292, 2016.

[3] M. Leary, "Surface roughness optimisation for selective laser melting (SLM)," in *Laser Additive Manufacturing*, pp. 99–118, Elsevier, Amsterdam, Netherlands, 2017.

[4] S. A. M. Tofail, E. P. Koumoulos, A. Bandyopadhyay, S. Bose, L. O'Donoghue, and C. Charitidis, "Additive manufacturing: scientific and technological challenges, market uptake and opportunities," *Materials Today*, vol. 21, no. 1, pp. 22–37, 2018.

[5] W. Gao, Y. Zhang, D. Ramanujan et al., "The status, challenges, and future of additive manufacturing in engineering," *Computer-Aided Design*, vol. 69, pp. 65–89, 2015.

[6] A. Gisario, M. Kazarian, F. Martina, and M. Mehrpouya, "Metal additive manufacturing in the commercial aviation industry: a review," *Journal of Manufacturing Systems*, vol. 53, pp. 124–149, 2019.

[7] K. Sherafatnia, G. H. Farrahi, and A. H. Mahmoudi, "Effect of initial surface treatment on shot peening residual stress field: analytical approach with experimental verification," *International Journal of Mechanical Sciences*, vol. 137, pp. 171–181, 2018.

[8] P. Zhang and Z. Liu, "Enhancing surface integrity and corrosion resistance of laser cladded Cr-Ni alloys by hard turning and low plasticity burnishing," *Applied Surface Science*, vol. 409, pp. 169–178, 2017.

[9] J. Sun, A. Su, T. Wang, W. Chen, and W. Guo, "Effect of laser shock processing with post-machining and deep cryogenic treatment on fatigue life of GH4169 super alloy," *International Journal of Fatigue*, vol. 119, pp. 261–267, 2019.

[10] J. Vaithilingam, R. D. Goodridge, R. J. M. Hague, S. D. R. Christie, and S. Edmondson, "The effect of laser remelting on the surface chemistry of Ti6al4V components fabricated by selective laser melting," *Journal of Materials Processing Technology*, vol. 232, pp. 1–8, 2016.

[11] A. Babu, H. S. Arora, R. B. Nair, I. Chakraborty, A. Chauhan, and H. S. Grewal, "Wear behavior of microwave-annealed and cryogenically treated thermal spray coatings: a comparative evaluation," *Materials Today: Proceedings*, vol. 33, pp. 5348–5353, 2020.

[12] E. Łyczkowska-Widłak, P. Lochyński, and G. Nawrat, "Electrochemical polishing of austenitic stainless steels," *Materials*, vol. 13, no. 11, pp. 1–25, 2020.

[13] A. Balyakin, E. Goncharov, and E. Zhuchenko, "The Effect of Preprocessing on Surface Quality in the Chemical Polishing of Parts from Titanium alloy Produced by SLM," *Materials Today: Proceedings*, vol. 19, pp. 2291–2294, 2019.

[14] G. Yang, B. Wang, K. Tawfiq, H. Wei, S. Zhou, and G. Chen, "Electropolishing of surfaces: theory and applications," *Surface Engineering*, vol. 33, no. 2, pp. 149–166, 2016.

[15] D. Landolt, "Fundamental aspects of electropolishing," *Electrochimica Acta*, vol. 32, no. 1, pp. 1–11, 1987.

[16] W. Han and F. Fang, "Fundamental aspects and recent developments in electropolishing," *International Journal of Machine Tools and Manufacture*, vol. 139, pp. 1–23, 2019.

[17] Y. Zhang, J. Li, S. Che, and Y. Tian, "Electrochemical polishing of additively manufactured Ti-6Al-4V alloy," *Metals and Materials International*, vol. 26, no. 6, pp. 783–792, 2020.

[18] N. C. Ferreri, D. J. Savage, and M. Knezevic, "Non-acid, alcohol-based electropolishing enables high-quality electron backscatter diffraction characterization of titanium and its alloys: application to pure Ti and Ti-6Al-4V," *Materials Characterization*, vol. 166, no. Aug, Article ID 110406, 2020.

[19] J. F. Moulder, W. F. Stickle, P. E. Sobol, and K. D. Bomben, *Handbook of X-ray Photoelectron Spectroscopy*, Perkin-Elmer Corporation, Massachusetts, USA, 1992.

[20] A. Acquesta and T. Monetta, "The electropolishing of additively manufactured parts in titanium: state of the art," *Advanced Engineering Materials*, vol. 23, no. 12, Article ID 2100545, 2021.

[21] M. E. Orazem and B. Tribollet, *Electrochemical Impedance Spectroscopy*, John Wiley & Sons, New Jersey, USA, 2008.